Thesis proposal: Rubidium Resonant Pulsed Polarization Squeezing

Yannick Alan de Icaza Astiz

ICFO - Institut de Ciencies Fotoniques, Mediterranean Technology Park, 08860 Castelldefels (Barcelona), Spain
UPC - Universitat Politècnica de Catalunya Barcelona Tech.

Thesis advisor: *Morgan W. Mitchell*

E-mail: Yannick.deIcaza@icfo.es

Abstract. Atomic magnetometers have become the most sensitive tools of measuring magnetic fields. New developments in this vibrant area of knowledge can lead to new technologies in the study of fast and small magnetic fields, such as the ones produced by the human brain. However, limitations of an atomic magnetometer that is probed using light are: atomic projection noise of the atoms and *shot noise* of the probing light. I propose to make, detect, characterize and apply a "fast-measuring" source to interact with Rubidium atoms: Rubidium-resonant pulsed polarization squeezed light. We prove in this work that it is theoretically possible to produce pulsed polarization squeezing using an optical parametric oscillator resonant to Rubidium and an acousto-optic modulator. From this calculation we conclude that one could have a repetition rate as high as 3 MHz of the pulses, still preserving a good degree of squeezing. In this way, we could improve the detection of fast and small magnetic fields, and measure them in an atomic magnetometer using the Faraday effect. This proposal is divided as follows: *context*, *objectives*, and *work plan and calendar*.

1. Context

The improvement of *sensitivity* and *time resolution* in the measurement of magnetic fields can lead to new applications in the study of fast and small fields, such as the ones produced by the human brain [1, 2]. Until 2003 super-conducting quantum interference devices (SQUIDs) were the top technology for ultra-high-sensitivity magnetometry – reaching a sensitivity of $\mathrm{fT}/\sqrt{\mathrm{Hz}}$, nowadays atomic magnetometers have taken this rank [3] –with a sensitivity below $\mathrm{fT}/\sqrt{\mathrm{Hz}}$. Optically-probed atomic magnetometers are based on readout of magnetic atomic ensembles. Rubidium based atomic magnetometers rely on the fact that an alkali atom has an unpaired electron in its outer shell whose spin rapidly precesses in an external magnetic field.

In 2008, Predojević *et al.* [4] produced rubidium-resonant squeezed light in our labs, which is a distinctive non-classical feature that has the property to reduce the

noise on the measurements –improvement of sensitivity–. In 2010, Wolfgramm *et al.* [5] demonstrated an optical magnetometer with sensitivity better than the shot-noise limit (fundamental source of noise that arises because the corpuscular character of the carriers) using a polarization-squeezed probe tuned near the atomic resonance. For doing time resolved measurements with high sensitivity, in this document, it is proposed to produce short pulses of polarization-squeezed light. Due to the pulses, fast oscillating magnetic fields could be resolved in time –improvement of time resolution–.

1.1. State of the art

1.1.1. Magnetoencephalography (MEG) When information is being processed by the brain, small currents flow in the neural system and produce a weak magnetic field which, nowadays, can be measured noninvasively by a SQUID magnetometer. A huge detector composed of flux-transformers (SQUIDs) and liquid helium for cooling is placed as close to the head of an human. This huge detector maps the magnetic field measured at each flux-transformer into data. But in the MEG interpretation data, one is dealing with the electromagnetic inverse problem, that is the deduction of the source currents responsible for the externally measured field. It is well known (Helmholtz 1853) that this problem has not unique solution, one way to give a solution to this problem is using source models, such as current dipoles.

The main emphasis on magnetoencephalography has been on basic research, for understanding the dynamics of the brain. Nevertheless, there are more and more papers on clinical studies that uses MEG as a technique to study diseases.

SQUID consists of two superconductors separated by thin insulating layers to form two parallel Josephson junctions –two superconductors separated by a thin insulating layer can experience tunneling of Cooper pairs of electrons through the junction–. SQUID magnetometer is classified within the flux methods of measuring magnetization of a sample. It measures magnetic flux through a pick-up loop (coil). This signal is proportional magnetic moment of a sample which is magnetized by the magnetic field produced by a superconducting magnet.

1.1.2. Atomic magnetometers. The limitations of an atomic magnetometer, one of the best magnetometers [3], that is probed using light are: atomic projection noise of the atoms and *shot noise* of the light [6, 7, 8]. I will focus on the second, there is a way to improve the sensitivity of an optically probed atomic magnetometer: a sub-shot-noise probe.

1.1.3. Optical parametric oscillator. An optical parametric oscillator (OPO) type-I –that produces one mode squeezed vacuum– is used to probe an atomic magnetometer. The vertically-polarized output beam is combined with the horizontally-polarized local oscillator (LO) at a polarizing beam splitter, see figure 1. This polarization-squeezed light is sent through an atomic cell, and is used to perform sub-shot-noise measurements

of a magnetic field by Faraday effect. Since a magnetic field creates a circular birefringence in the vapor due to Zeeman effect.

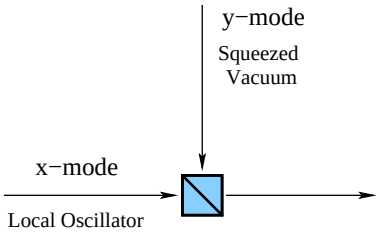

Figure 1. Polarization combination of local oscillator and squeezed vacuum.

1.1.4. Rubidium resonant squeezed light. Predojević *et al.* [4] used as principal light source an external-cavity diode laser at 794.7 nm, tunable over the D1 transition of rubidium. The output is amplified using a tapered amplifier and is split in two parts. (a) The weaker part is used as local oscillator, and (b) the stronger is frequency doubled to 397.4 nm and sent through a single-mode fiber obtaining ∼42 mW that are used to pump a sub-threshold optical parametric oscillator (OPO). The nonlinear medium of the OPO is a type-I PPKTP crystal. The OPO generates squeezed coherent states at 794.7 nm, because of the nonlinear effect. They stabilize actively the cavity using a frequency-shifted beam with a polarization orthogonal to the polarization of the squeezed vacuum. The light produced can have up to -3 dB of squeezing.

Definition 1 (Quadrature squeezing) *Means that the level of quantum fluctuations of one quadrature component (X^+ or X^-) is less than level corresponding to the coherent state ($V_{X^+} = V_{X^-} = 1$). Mathematically*

$$V_{X^+} < 1 \quad \text{or} \quad V_{X^-} < 1. \tag{1}$$

Where V_A is the variance of the operator A defined by

$$V_A \equiv \langle (\Delta \hat{A})^2 \rangle \equiv \langle \hat{A}^2 \rangle - \langle \hat{A} \rangle^2. \tag{2}$$

And finally $\hat{X}^+$, $\hat{X}^-$ are the quadrature operators, see definition 2 for details.

Following the definition of quadrature squeezing we obtain the figure 2.

1.1.5. Why not try to combine a good atomic system with a good probe technology? In this proposal I will be focused on the probe system, a pulsed-polarization squeezed beam, following the recently paper from our group [5], where they used a polarization-squeezed probe. A good atomic system could be the one presented in [9], also from our group. In the end, with light pulses with a repetition rate up to ∼ 3 MHz, we can measure fields that have a lower repetition rate with great accuracy.

1.1.6. ***Competing techniques***

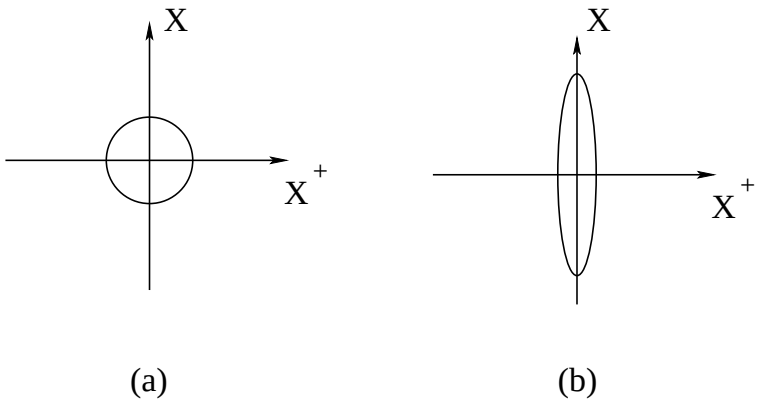

Figure 2. Example of Quadrature Squeezing. Uncertainty circle/ellipse for (a) coherent state (output from a standard laser) and (b) squeezed state.

SQUID magnetometers vs atomic magnetometers. In contrast to SQUIDs, which require cooling with liquid helium (4.2^{o} K) or liquid nitrogen (77^{o} K) to operate, atomic magnetometers have the intrinsic advantage of not requiring cryogenic cooling. Another advantage is that they measure the magnetic field directly, allowing them to detect other spin interactions. While the SQUIDs measure magnetic flux through a pick-up loop. Quite recently, Taue *et al.* [10] developed a highly sensitive optically pumped atomic magnetometer for measuring biomagnetic fields. The sensitivity of the magnetometer reached up to 10 fT/$\sqrt{\text{Hz}}$. There is still work to be done to reach a sub-fT sensitivity.

Rubidium-resonant pulsed polarization squeezing. Heersink *et al.* [11] have generated polarization squeezing of pulses in the past (other people [12, 13] are also working in the field using other techniques: four-wave mixing, nonlinear rotation of the polarization ellipse in a Rb vapor). They have used an asymmetric fiber-optic Sagnac interferometer. The Kerr nonlinearity of the fiber was exploited to produce independent amplitude squeezed pulses. The pulses ($\sim$ 150 fs) were produced using a Cr^{4+}:YAG passive Q-switch crystal at 1495 nm. This light it is not atom-resonant and each pulse has a bandwidth of 2.9 THz. The way we would produce pulses of squeezed light it is more advantageous to do rubidium interactions because the bandwidths of the proposed-pulses ($\sim$ 1.5 MHz) are short compare the resonant lines rubidium ($\sim$ 300 MHz including Doppler broadening). For example using the pulses from [11] (150 fs) we have a bandwidth of 2.9 THz. This kind of pulse is a broadband pulse and it is not good for atom interaction. Because the pulse can interact with two hyperfine levels or more, and prevents to optically readout a well-defined state.

1.2. **Potential impact.**

Concerning the potential improvement in the detection of magnetic fields, fast and sensitive measurements can lead to the development of new technology. There is a direct impact on other fields, detecting the magnetic fields produced by the heart:

magnetocardiology [14]; and the brain: magnetoencephalography [15]. A source of rubidium-resonant pulsed polarization squeezing could improve the sensitivity of the measurements of the rubidium magnetometers [10]. Also there is a potential impact on the measurement of the geomagnetic anomalies [3].

A source of pulsed-polarization-squeezing could have a direct application in the work of Koschorreck *et al.* [9]. They have already a good atomic magnetometer: a cold, dipole-trapped sample of rubidium atoms provides a long-lived spin system in a non-magnetic environment, and is probed nondestructively by paramagnetic Faraday rotation, using "normal" pulses. Instead, if they could use squeezed pulses they could improve their results in the order of the squeezing.

2. Objectives

The aim of this thesis is to **make** (see 2.1), **detect** (see 2.2), **characterize** (see 2.3 and 2.4), and later **apply** (see 2.5) a new source of light, resonant with Rubidium, that can enhance sensitivity (squeezed light) and improve time resolution (pulsed light) of measurements.

2.1. Generation of pulsed polarization squeezing

My proposal is based on the actual experimental setup that is summarized in previous publications [4, 5]. The idea is to introduce an *acousto-optic modulator* (AOM) to modulate the local oscillator, in this way the squeezed vacuum light generated after the OPO will be combined with a pulsed local oscillator at the first polarization beam splitter (PBS1), see figure 3.

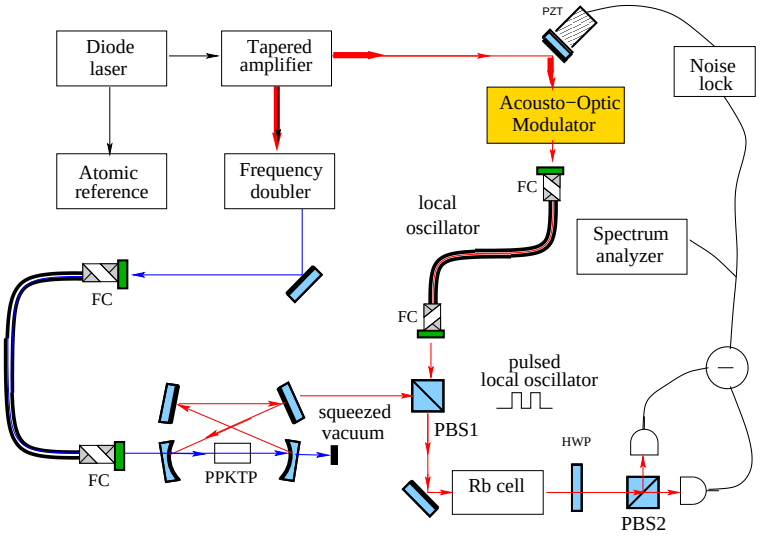

Figure 3. Experimental setup for generation and detection of pulsed polarization squeezing. Rb cell, rubidium vapor cell; PPKTP, phase-matched nonlinear crystal; FC, fiber coupling; PBS, polarizing beam splitter; HWP, half-wave plate. PZT, piezoelectric transducer.

Using a commercial AOM (Neos 46080-2) it is possible to obtain pulses as short as 300 ns. Because the rise time of the AOM is $t_{\text{rise}} = \frac{150 \text{ ns}}{\text{beam dia [mm]}}$, for a beam of 1 mm, that has still a good efficiency $\sim 50\%$, we have a pulse of 300 ns, assuming that the fall time is the same as the rise time, that in practice is true.

These limit-pulses have a repetition rate of 3.3 MHz, though we can tune the repetition rate of the AOM from DC up to this limit frequency. In the end, having tunable pulses is like having a strobe. So we can measure fields with our strobe, and thus detect fast phenomena.

2.2. **Detection of pulsed polarization squeezing**

We have detected before quadrature squeezing and polarization squeezing in our labs. But, in order to detect a pulsed (squeezed) beam we need to do a careful analysis.

The fundamental source of noise, the (optical) shot noise ΔP_{shot} [W] is

$$\Delta P_{shot} = \sqrt{2h\nu \bar{P} B} \tag{3}$$

Where h is the Plank constant, ν the frequency of the beam and $\bar{P}$ is the average optical power of the beam. The bandwidth of the detector is the difference between the upper and lower frequencies in a continuous set of frequencies that are sent to the detector.

The second source of noise is the *thermal* or *Johnson noise* $\Delta I_{thermal}$. There is another shot-noise contribution, *dark noise* (ΔI_{dark}), for the noise that produces the dark current I_{dark}, current produced in the absence of light in the detector.

The total noise is

$$\Delta I_{tot} = \sqrt{\Delta I_{shot}^2 + \Delta I_{dark}^2 + \Delta I_{thermal}^2}. \tag{4}$$

A detector for which $\Delta I_{electronic}^2 = \Delta I_{dark}^2 + \Delta I_{thermal}^2 \leq \Delta I_{shot}^2$ is named "shot-noise-limited". Because the noise is going to be limited by the light, or in other words we can detect the noise created by the light, because we are not limited by the electronic noise.

2.2.1. Detecting pulses A balanced-amplified detector (Thorlabs PDB150) with switchable-gain was used to detect squeezing in our lab. Transimpedance gain can be set by a five position rotary switch from $10^3 - 10^7$ V/A. This detector has the bandwidths of $B = 0.1, 0.3, 5, 50, 150$ MHz.

The one-sided power spectral density of the optical power in the case of shot noise is $PSD_{optical} = 2h\nu\bar{P}$ [W^2/Hz] [16]. The shot noise per square root of bandwidth is $\Delta P_{shot/\sqrt{B}} = \sqrt{PSD_{optical}}$ [W/$\sqrt{\text{Hz}}$].

Predojević [4, 17] measured the noise of our detector finding that the electronic noise of the whole system with 400 μW of input power was 14 dB below the shot-noise limit. This result is consistent with this calculations.

It is possible to use this detector to detect pulsed light, since the detector has different bandwidths. An AOM can be used to produce pulses as short as 300 ns, that

$\bar{P}$ [mW]	$\Delta P_{shot/\sqrt{B}}$ [pW/$\sqrt{\text{Hz}}$]
0.4	14.14
0.1	7.069
0.001	0.707
0.0008	0.6323

The noise equivalent power reported by the manufacturer is 0.6 pW/$\sqrt{\text{Hz}}$. *Therefore our detector is shot noise limited for powers higher that 0.8* μW.

Table 1. Shot noise per $\sqrt{B}$ ($\Delta P_{shot/\sqrt{B}}$) vs optical power ($\bar{P}$)

implies a bandwidth $B = 1.47$ MHz for Gaussian pulses. It was tested, already, that the detector is shot-noise limited up to 5 MHz [4, 17]. The same spectrum analyzer can be used to detect pulses if the detector has the sufficient bandwidth.

2.3. Theory of pulsed polarization squeezing

In this section and the next one, I will characterize some features of "pulsed polarization squeezed light". First, I will check that the quadrature squeezing produced in the optical parametric oscillator is transferred into the pulses in form of polarization squeezing. As a theoretical calculation, it requires all the elements to be correct. The full calculation is in Appendix A. Secondly, we need to relate the quantum theory with the signals that can be measured. For doing this, I will write the correlation functions (see section 2.4), that bonds the subtracted current that could be detected with the operators, moreover with its variance in a time-window.

As shown in Appendix A, when a state with zero average field is combined with a strong coherent state of the orthogonal polarization, quantum features of the quadrature variables are transferred onto the polarization variables. Each pulse satisfies the definition of polarization squeezing.

2.4. Correlation functions

In a single mode description, the homodyne current (the subtracted current from the two detectors on figure 3) is

$$\Delta\mathcal{I} \propto \langle \hat{p}^\dagger \hat{s} + \hat{s}^\dagger \hat{p} \rangle. \tag{5}$$

Where $\hat{p}$ is the operator from the local oscillator and $\hat{s}$ is the operator of the squeezed light.

The multi-mode homodyne current is.

$$\Delta I(t) \propto \left\langle \sum_{j=1}^{\infty}\sum_{l=1}^{\infty} e^{it(\omega_l-\omega_j)} \hat{p}_j s_l^\dagger + \sum_{\delta=1}^{\infty}\sum_{\kappa=1}^{\infty} e^{it(\omega_\delta-\omega_\kappa)} s_\kappa \hat{p}_\delta^\dagger \right\rangle. \tag{6}$$

Where, in this case, $\hat{p}$ is the operator from the pulsed local oscillator, and ω is the frequency.

I will calculate the expectation value from the variance in a window 2τ.

$$\Pi(\Delta I) \equiv \left\langle \int_{-\tau}^{\tau} \int_{-\tau}^{\tau} \Delta I(t')\Delta I(t'')dt'dt'' \right\rangle \tag{7}$$

The full calculation is in Appendix B, the result is in terms of the variables $\Omega \equiv \frac{\omega}{\delta}$ –detection frequency– and $\xi \equiv \delta \cdot \Omega$; with the parameters δ as the cavity linewidth, 2τ as the pulse width, and μ as the pumping parameter. The result from the calculation can be summarized as the anti-squeezing:

$$\Pi(\Delta I) = 4|\alpha|^2 \sum_l \frac{\sin^2(\xi_l \tau)}{\xi_l^2}\left(1 + \frac{4\mu}{(1-\mu)^2 + \Omega_l^2}\right). \tag{8}$$

And the squeezing:

$$\Pi(\Delta I) = 4|\alpha|^2 \sum_l \frac{\sin^2(\xi_l \tau)}{\xi_l^2}\left(1 - \frac{4\mu}{(1+\mu)^2 + \Omega_l^2}\right). \tag{9}$$

It was assumed that the amplitude of the local oscillator α is $|\alpha|^2 \gg 1$, for neglecting a background term that is not going to be amplified by the local oscillator.

For plotting (see figure 4) these equation (for one Ω_l) we assume $\mu = \sqrt{\frac{1}{2}}$. The reference line is obtained by putting $\mu = 0$ (no squeezing).

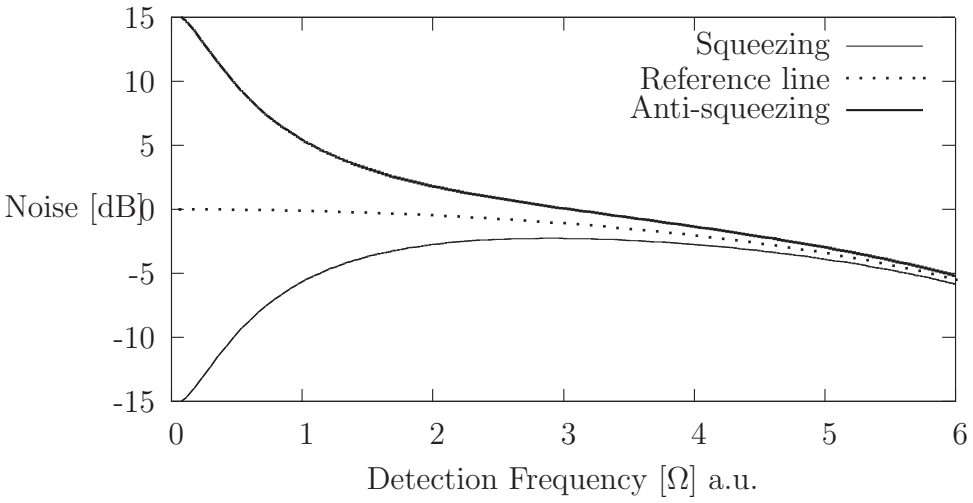

Figure 4. Spectral dependence of the squeezing and anti-squeezing in pulses produced by an optical parametric oscillator and acousto-optic modulator.

The last equation of this proposal is to quantify the squeezing that can be obtained, the **Degree of Squeezing** (DoS) is

$$DoS \equiv \frac{\int_{-\infty}^{\infty} \frac{sin(\delta\tau\Omega)^2}{(\delta\tau\Omega)^2}\left(1 - \frac{4\mu}{(1+\mu)^2+\Omega^2}\right)d\Omega}{\int_{-\infty}^{\infty} \frac{sin(\delta\tau\Omega)^2}{(\delta\tau\Omega)^2}d\Omega}. \tag{10}$$

Pulse width 2τ	DoS	Pulse width 2τ	DoS
2 ns	0.98	200 ns	0.30
20 ns	0.85	600 ns	0.13

Table 2. Degree of Squeezing (DoS) obtained for different pulse widths 2τ.

As shown in the figure 4, the squeezing and anti-squeezing are very different in the origin of the detection frequency, but they approach asymptotically to the reference curve. Table 2 shows that there is a good degree of squeezing DoS for pulses in the order of 200 ns, the pulses that are very short lose the squeezing. The pulsed duration compromises the transfer of the squeezing in the pulse. Still pulses with repetition rates as high as 3 MHz can have good squeezing. And therefore, we can detect processes that happen with repetition rates as high as 3 MHz, the approximate limit of the acousto-optic modulator.

2.5. Squeezing-enhanced magnetometry

When we have a source of pulsed-polarization-squeezing we want to measure magnetic fields using the setup summarized in figure 3.

3. Work plan and calendar

3.1. Previous work related

In spring-summer 2009 (5-6 months including writing and presentation), I worked in my master project "*Binary coherent beam combining with semiconductor tapered amplifiers at 795 nm*" [18]. In this work, I acquired the necessary knowledge to work with semiconductor lasers and taperd amplifiers. I was able to design pieces, to work with temperature controllers and laser drivers, I also designed a locking and stabilization system of the optical power.

From autumn 2009, I was mainly focused in the thesis proposal. First I was working to try to "squeezed spontaneous emission", but a paper from Kimble's group revealed that the project was too ambitious, because of the methods and techniques that need to be developed before to work on this subject. At this period I also worked with A. Cerè in a "Polarization-independent narrowband filter based on velocity-selective optical pumping in Rubidium vapor".

From spring 2010, I started to work in a new *project* and later in the *theory* of "pulsed polarization squeezing". I also worked with F. A. Beduini in a heating system that changes the optical density of a Rubidium cell that has been applied in [19].

In fall 2010, I tested the electronics components that are needed to work with an AOM. And I also finish the theory of this proposal.

With this background in electronics (oscilloscopes, laser drivers, temperature controllers, spectrum analyzer, stabilization and locking systems) and in laser technology

(atomic references –spectroscopy–, semiconductor lasers and tapered amplifiers) I propose the following work plan.

3.2. Work plan and calendar

(i) Producing pulses with an (two) AOM(s). *2 month.*
   (a) Bibliography
   (b) Test the electronic items (voltage controller oscillator, amplifier, logic switch).
   (c) Characterization of pulses.

(ii) Shot-noise limited detection. *1 month.*
   Measure the noise using pulses and the balanced thorlabs detector.

(iii) Producing polarization squeezing. *1 month.*
   (a) Facilities: Tapered amplifier, spectrum analyzer, cavity stabilization.
   (b) Measure the actual polarization squeezing.

(iv) Producing pulsed polarization squeezing. *4 months.*
   (a) Introduce the AOM into the local oscillator of the squeezing system.
   (b) Design mechanical pieces if needed.
   (c) Measure the pulsed polarization squeezing.
   (d) Adjust the noise lock, try to use the actual one with modification on the parameters, or build a custom solution.

(v) Squeezing-enhanced magnetometry. *5 months.*
   (a) Bibliography.
   (b) Prepare Rubidium cells with different buffer gas pressures.
   (c) Measure the intensity saturation and the optical density of the different cells.
   (d) Improve, if needed, the mechanical system that holds and heats the cells.
   (e) Construct coils to produce magnetic fields to characterize afterwards.
   (f) Implement a system that can produce magnetic fields that oscillate with frequencies lower than 3 MHz.
   (g) Measure magnetic fields using a pulsed-squeezed-polarization source.
   (h) Use the pulses as a strobe and probe the magnetic fields.

(vi) Other applications *6 months.*

(vii) Writing the thesis. *3 months.*

References

[1] I. K. Kominis, T. W. Kornack, J. C. Allred, and M. V. Romalis. A subfemtotesla multichannel atomic magnetometer. *Nature*, 422(6932):596–599, 2003.

[2] Matti Hämäläinen, Riitta Hari, Risto J. Ilmoniemi, Jukka Knuutila, and Olli V. Lounasmaa. Magnetoencephalography–theory, instrumentation, and applications to noninvasive studies of the working human brain. *Rev. Mod. Phys.*, 65(2):413–, April 1993.

[3] D. Budker and M. Romalis. Optical magnetometry. *Nature Physics*, 3:227–234, 2007.

[4] A. Predojević, Z. Zhai, J. M. Caballero, and M. W. Mitchell. Rubidium resonant squeezed light from a diode-pumped optical-parametric oscillator. *Phys. Rev. A*, 78(6):063820–, December 2008.

[5] Florian Wolfgramm, Alessandro Cerè;, Federica A. Beduini, Ana Predojević, Marco Koschorreck, and Morgan W. Mitchell. Squeezed-light optical magnetometry. *Phys. Rev. Lett.*, 105(5):053601–, July 2010.

[6] M. Auzinsh, D. Budker, D. F. Kimball, S. M. Rochester, J. E. Stalnaker, A. O. Sushkov, and V. V. Yashchuk. Can a quantum nondemolition measurement improve the sensitivity of an atomic magnetometer? *Phys. Rev. Lett.*, 93(17):173002–, October 2004.

[7] I. K. Kominis. Sub-shot-noise magnetometry with a correlated spin-relaxation dominated alkali-metal vapor. *Phys. Rev. Lett.*, 100(7):073002–, February 2008.

[8] V. Shah, G. Vasilakis, and M. V. Romalis. High bandwidth atomic magnetometery with continuous quantum nondemolition measurements. *Phys. Rev. Lett.*, 104(1):013601–, January 2010.

[9] M. Koschorreck, M. Napolitano, B. Dubost, and M. W. Mitchell. Sub-projection-noise sensitivity in broadband atomic magnetometry. *Phys. Rev. Lett.*, 104(9):093602–, March 2010.

[10] S. Taue, Y. Sugihara, T. Kobayashi, S. Ichihara, K. Ishikawa, and N. Mizutani. Development of a highly sensitive optically pumped atomic magnetometer for biomagnetic field measurements: A phantom study. *Ieee Transactions On Magnetics*, 46(9):3635–3638, September 2010.

[11] J. Heersink, T. Gaber, S. Lorenz, O. Glockl, N. Korolkova, and G. Leuchs. Polarization squeezing of intense pulses with a fiber-optic sagnac interferometer. *Physical Review A*, 68(1):013815, July 2003.

[12] Imad H. Agha, Gaetan Messin, and Philippe Grangier. Generation of pulsed and continuous-wave squeezed light with rb-87 vapor. *Optics Express*, 18(5):4198–4205, MAR 1 2010.

[13] J. Appel, E. Figueroa, M. Korystov, D.and Lobino, and A. I. Lvovsky. Quantum memory for squeezed light. *Phys. Rev. Lett.*, 100(9):093602–, March 2008.

[14] G. Bison, R. Wynands, and A. Weis. A laser-pumped magnetometer for the mapping of human cardiomagnetic fields. *Applied Physics B-Lasers And Optics*, 76(3):325–328, 2003.

[15] H. Xia, A. B. A. Baranga, D. Hoffman, and M. V. Romalis. Magnetoencephalography with an atomic magnetometer. *Applied Physics Letters*, 89(21):211104, 2006.

[16] Rüdiger Paschotta. *Encyclopedia of Laser Physics and Technology*. Wiley-VCH, 2008.

[17] A. Predojević. *Rubidium resonant squeezed light from a diode-pumped optical-parametric oscillator*. PhD thesis, ICFO-UPC, 2009.

[18] Yannick Alan de Icaza Astiz. Binary coherent beam combining with semiconductor tapered amplifiers at 795 nm. Master's thesis, Msc in Photonics. UPC Barcelona Tech, 2009.

[19] F. Wolfgramm, Yannick A. de Icaza Astiz, F. A. Beduini, A. Cerè, and M. W. Mitchell. Atom-resonant heralded single photons by interaction-free measurement. To appear in Phys. Rev. Lett.

Appendix A. Formal proof: *Quadrature squeezing* plus an AOM implies *pulsed polarization squeezing*

For the formal proof, I will need, firstly the definitions of *quadrature squeezing*, *quadrature operators*, *Stokes operators*, and *the generalized uncertainty principle* to motivate the definition of *polarization squeezed state*. Secondly, the commutator relations, thirdly a way to split the operator into "classical amplitude" plus a "noise operator", and the rest is algebra of operators.

Definition 2 (Quadrature operators *and* generalized quadrature operator) *The quadrature operators ($\hat{X}_j^+$, $\hat{X}_j^-$) of mode j, in terms of the creation $\hat{a}_j^\dagger$ and annihilation $\hat{a}_j$ ($\hat{a}_j$ and $\hat{a}_j^\dagger$ satisfy the commutation relations $[\hat{a}_j, \hat{a}_k^\dagger] = \delta_{jk}$, $[\hat{a}_j^\dagger, \hat{a}_k^\dagger] = 0$, $[\hat{a}_j, \hat{a}_k] = 0$) are*

$$\hat{X}_j^+ \equiv \hat{a}_j^\dagger + \hat{a}_j, \quad \hat{X}_j^- \equiv i(\hat{a}_j^\dagger - \hat{a}_j), \quad j = x, y. \tag{A.1}$$

The generalized quadrature operator is:

$$X_j(\theta) \equiv X_j^+ \cos\theta + X_j^- \sin\theta. \tag{A.2}$$

Remark 1 *The commutation relation of the quadrature operators ($\hat{X}_j^+$, $\hat{X}_k^-$) is*

$$[\hat{X}_j^+, \hat{X}_k^-] = 2i\delta_{jk}. \tag{A.3}$$

In order to produce polarization squeezing we combine the local oscillator and the quadrature squeezed in a polarization beam splitter (PBS), see figure 1. The **Stokes operators** describe the polarization state after the PBS, written in terms of the creation $\hat{a}_{x/y}^\dagger$ and annihilation $\hat{a}_{x/y}$ operators of two orthogonal modes x and y.

$$\begin{aligned} \hat{S}_0 &\equiv \hat{a}_x^\dagger \hat{a}_x + \hat{a}_y^\dagger \hat{a}_y, \\ \hat{S}_1 &\equiv \hat{a}_x^\dagger \hat{a}_x - \hat{a}_y^\dagger \hat{a}_y, \\ \hat{S}_2 &\equiv \hat{a}_x^\dagger \hat{a}_y + \hat{a}_y^\dagger \hat{a}_x, \\ \hat{S}_3 &\equiv i\big(\hat{a}_y^\dagger \hat{a}_x - \hat{a}_x^\dagger \hat{a}_y\big). \end{aligned} \tag{A.4}$$

The $\hat{S}_0$ corresponds to the total coherent excitation, whilst the others describe the polarization state. The $\hat{S}_0$ operator commutes with the others: $[\hat{S}_0, \hat{S}_j] = 0, \quad j = 1, 2, 3$, whereas the remaining operators satisfy the commutator:

$$[\hat{S}_1, \hat{S}_2] = 2i\hat{S}_3, \tag{A.5}$$

and the cyclic ones thereof.

Theorem 1 (The generalized uncertainty principle)
If two operators $\hat{A}$ and $\hat{B}$ satisfy the commutation relation $[\hat{A}, \hat{B}] = i\hat{C}$, it follows that

$$V_A V_B \geq \frac{1}{4}|\langle C \rangle|^2. \tag{A.6}$$

The commutator A.5 leads (from the theorem 1) to a restriction on the means and variances by uncertainty relations.

$$V_1 V_2 \geq |\langle \hat{S}_3 \rangle|^2, \quad V_3 V_1 \geq |\langle \hat{S}_2 \rangle|^2, \quad V_2 V_3 \geq |\langle \hat{S}_1 \rangle|^2. \tag{A.7}$$

Where $V_j \equiv V_{S_j}$ and V_{S_j} is defined in 2. This give rise to the formal definition of a polarization squeezed state, in analogy to definition 1.

Definition 3 (Polarization squeezed state) *A state is called* polarization squeezed *if*

$$V_j < |\langle \hat{S}_k \rangle|, \quad j \neq k. \tag{A.8}$$

An intuitive definition of a polarization squeezed state is a quantum state of light in which the level of quantum fluctuations of one Stokes operator lies below the level corresponding to the coherent polarization state.

The quantum description of the output of an Acousto-Optic Modulator (AOM) is similar to the description of a Beam Splitter (BS). We have that the x-mode in the figure 1 is

$$\hat{a}_x(t) = R(t)\hat{a}_1 + T(t)\hat{a}_0. \tag{A.9}$$

Where the 1-mode is a coherent state, the 0-mode is a vacuum state, $R(t)$ and $T(t)$ are the reflectance and the transmittance that must satisfy the following relations: $|R|^2 + |T|^2 = 1$, and $R^*T - RT^* = 0$, in order to satisfy the commutation relations.

We can write $\hat{a}_j$ as **classical amplitude** or **coherent excitation** α_j plus the **noise operator** $\delta\hat{a}_j$. We can observe that $\langle\alpha_j|\delta\hat{a}_j|\alpha_j\rangle = 0$. In this notation $\hat{a}_1 = \alpha_1 + \delta\hat{a}_1$ and $\hat{a}_0 = \delta\hat{a}_0$. The y-mode $\hat{a}_y$ will be $\lim_{\alpha_2\to 0}\alpha_2 + \delta\hat{a}_2$.

In this notation with $R \equiv R(t)$ and $T \equiv T(t)$, the Stokes parameters become:

$$\begin{aligned}
\hat{S}_0 &= R^2\alpha_1^2 + \alpha_2^2 + R^2\alpha_1\delta X_1^+ + \alpha_2\delta X_2^+ + \alpha_1 RT\delta X_0^+, \\
\hat{S}_1 &= R^2\alpha_1^2 - \alpha_2^2 + R^2\alpha_1\delta X_1^+ - \alpha_2\delta X_2^+ + \alpha_1 RT\delta X_0^+, \\
\hat{S}_2 &= 2R\alpha_1\alpha_2\cos\phi + \alpha_1 R\delta X_2(-\phi) + \alpha_2(T\delta X_0(\phi) + R\delta X_1(\phi)), \\
\hat{S}_3 &= 2R\alpha_1\alpha_2\sin\phi + \alpha_1 R\delta X_2(\tfrac{\pi}{2} - \phi) + \alpha_2(T\delta X_0(\phi - \tfrac{\pi}{2}) + R\delta X_1(\phi - \tfrac{\pi}{2})).
\end{aligned} \tag{A.10}$$

Where $\delta\hat{X}_j^+ \equiv \delta\hat{a}_j^\dagger + \delta\hat{a}_j$, $\delta\hat{X}_j^- \equiv i(\delta\hat{a}_j^\dagger - \delta\hat{a}_j)$ are the quadrature-noise operators, and the generalized quadrature-noise operator is $\delta X_j(\theta) \equiv \delta X_j^+\cos\theta + \delta X_j^-\sin\theta$.

The mean values of A.10 are:

$$\begin{aligned}
\langle\hat{S}_0\rangle &= \alpha_1^2R^2 + \alpha_2^2, \qquad \langle\hat{S}_1\rangle = \alpha_1^2R^2 - \alpha_2^2, \\
\langle\hat{S}_2\rangle &= 2R\alpha_1\alpha_2\cos\phi, \quad \langle\hat{S}_3\rangle = 2R\alpha_1\alpha_2\sin\phi.
\end{aligned} \tag{A.11}$$

From A.10, I will compute the variances of the Stokes parameters.

$$\begin{aligned}
V_0 &= \alpha_1^2R^4\langle(\delta X_1^+)^2\rangle + \alpha_2^2\langle(\delta X_2^+)^2\rangle + \alpha_1^2(RT)^2\langle(\delta X_0^+)^2\rangle \\
V_1 &= \alpha_1^2R^4\langle(\delta X_1^+)^2\rangle + \alpha_2^2\langle(\delta X_2^+)^2\rangle + \alpha_1^2(RT)^2\langle(\delta X_0^+)^2\rangle \\
V_2 &= \alpha_1^2R^2\langle(\delta X_2(-\phi))^2\rangle + \alpha_2^2T^2\langle(\delta X_0(\phi))^2\rangle + \alpha_2^2R^2\langle(\delta X_1(\phi))^2\rangle \\
V_3 &= \alpha_1^2R^2\langle(\delta X_2(\tfrac{\pi}{2} - \phi))^2\rangle + \alpha_2^2T^2\langle(\delta X_0(\phi - \tfrac{\pi}{2}))^2\rangle + \alpha_2^2R^2\langle(\delta X_1(\phi - \tfrac{\pi}{2}))^2\rangle
\end{aligned} \tag{A.12}$$

For the case $\phi = 0$ they will become

$$\begin{aligned}
V_0 &= \alpha_1^2R^4V_{\delta X_1^+} + \alpha_2^2V_{\delta X_2^+} + \alpha_1^2(TR)^2V_{\delta X_0^+}, \\
V_1 &= \alpha_1^2R^4V_{\delta X_1^+} + \alpha_2^2V_{\delta X_2^+} + \alpha_1^2(TR)^2V_{\delta X_0^+}, \\
V_2 &= \alpha_1^2R^2V_{\delta X_2^+} + \alpha_2^2T^2V_{\delta X_0^+} + \alpha_2^2R^2V_{\delta X_1^+}, \\
V_3 &= \alpha_1^2R^2V_{\delta X_2^-} + \alpha_2^2T^2V_{\delta X_0^-} + \alpha_2^2R^2V_{\delta X_1^-}.
\end{aligned} \tag{A.13}$$

Where $V_{\delta\hat{X}_j^{+/-}}$ is (the variance) $\langle(\delta\hat{X}_j^{+/-})^2\rangle - \langle\delta\hat{X}_j^{+/-}\rangle^2 = \langle(\delta\hat{X}_j^{+/-})^2\rangle$.

The 0-mode and 1-mode are vacuum and coherent states, respectively, then $V_{\delta\hat{X}_1^+} = V_{\delta\hat{X}_1^-} = V_{\delta\hat{X}_0^+} = V_{\delta\hat{X}_0^-} = 1$. The 2-mode is a quadrature squeezed state $V_{\delta\hat{X}_2^+} < 1$, $V_{\delta\hat{X}_2^-} > 1$.

$$\begin{aligned}
V_0 &= \alpha_1^2R^2 + \alpha_2^2V_{\delta X_2^+}, \\
V_1 &= \alpha_1^2R^2 + \alpha_2^2V_{\delta X_2^+}, \\
V_2 &= \alpha_1^2R^2V_{\delta X_2^+} + \alpha_2^2. \\
V_3 &= \alpha_1^2R^2V_{\delta X_2^-} + \alpha_2^2.
\end{aligned} \tag{A.14}$$

Finally, using A.11, A.14 and $\lim_{\alpha_2\to 0}$ we can satisfy definition 3 ($V_2 < |\langle S_1\rangle|$) as

$$\begin{array}{ccc} \lim_{\alpha_2\to 0}(\alpha_1^2R^2V_{\delta X_2^+}+\alpha_2^2) & < & \lim_{\alpha_2\to 0}(\alpha_1^2R^2-\alpha_2^2) \\ \alpha_1^2R^2V_{\delta X_2^+} & < & \alpha_1^2R^2 \end{array} \tag{A.15}$$

Whenever $R(t)\neq 0$, because $V_{\delta\hat{X}_2^+}<1$. ■

Appendix B. Calculation of $\Pi(\Delta I)$

From 6 we apply the quantum description of the output of an Acousto-Optic Modulator A.9, as follows $\hat{p}=R\hat{a}+T\hat{c}$, we obtain

$$\Delta I(t)\equiv\Big\langle\sum_{j=1}^{\infty}\sum_{l=1}^{\infty}e^{it(\omega_l-\omega_j)}\left(R\hat{a}_j+T\hat{c}_j\right)s_l^\dagger+\sum_{\delta=1}^{\infty}\sum_{\kappa=1}^{\infty}e^{it(\omega_\delta-\omega_\kappa)}s_\kappa\left(R^*\hat{a}_\delta^\dagger+T^*\hat{c}_\delta^\dagger\right)\Big\rangle.$$

Where $\hat{a},\hat{s},\hat{c}$ are the operators from the coherent state, squeezed state and vacuum state, respectively. I will calculate the expectation value from the variance in a window 2τ. The state $|\Psi\rangle$ is $|\alpha_{\hat{a}},0_{\hat{s}},0_{\hat{c}}\rangle$, the modes $\hat{a},\hat{s},\hat{c}$ commutes. Firstly, I will calculate $\Delta I_\alpha^2\equiv\langle 0_{\hat{c}},\alpha_{\hat{a}}|\Delta I(t')\Delta I(t'')|\alpha_{\hat{a}},0_{\hat{c}}\rangle$, and later $\int_{-\tau}^{\tau}\int_{-\tau}^{\tau}\langle 0_{\hat{s}}|\Delta I_\alpha^2|0_{\hat{s}}\rangle dt'dt''$.

$$\Delta I_\alpha^2=|R|^2|\alpha|^2\sum_{l,\kappa}\Big(s_l^\dagger s_\kappa^\dagger e^{-i(t'(\omega_\alpha-\omega_l)+t''(\omega_\alpha-\omega_\kappa))}e^{2i\phi}+s_ls_\kappa e^{i(t'(\omega_\alpha-\omega_l)+t''(\omega_\alpha-\omega_\kappa))}e^{-2i\phi}$$
$$+s_l^\dagger s_\kappa e^{i(t''-t')(\omega_l-\omega_\kappa)}+s_\kappa s_l^\dagger e^{i(t''-t')(\omega_\kappa-\omega_l)}\Big)+\sum_{l,\kappa}s_l^\dagger s_\kappa e^{i(t''-t')(\omega_l-\omega_\kappa)}$$

Where it was used $R=|R|e^{i\zeta},\alpha=|\alpha|e^{i\chi}$, and $\phi=\xi+\zeta$.

Now, I will simplify this last equation using the commutator $[s_\kappa,s_l^\dagger]=\delta(\omega_\kappa-\omega_l)$, then I will calculate $\int_{-\tau}^{\tau}\int_{-\tau}^{\tau}\langle 0_{\hat{s}}|\Delta I_\alpha^2|0_{\hat{s}}\rangle dt'dt''$. Using $\hat{s}_\kappa=f_1\hat{b}_\kappa+f_2\hat{b}_{-\kappa}$. The parameters f_1,f_2 are described in Ana's thesis [17].

$$\Pi(\Delta I)=\int_{-\tau}^{\tau}\int_{-\tau}^{\tau}\Big[|\alpha|^2|R|^2\sum_l\Big(f_1^*(\Omega_l)f_2^*(\Omega_l)e^{-i(t'+t'')(\omega_\alpha-\omega_l)}e^{2i\phi}+f_1(\Omega_l)f_2(\Omega_l)e^{i(t'+t'')(\omega_\alpha-\omega_l)}e^{-2i\phi}$$
$$+1+2f_2^*(\Omega_l)f_2(\Omega_l)e^{i(t''-t')(\omega_\alpha-\omega_l)}\Big)+\sum_l f_2^*(\Omega_l)f_2(\Omega_l)e^{i(t''-t')(\omega_\alpha-\omega_l)}\Big]dt'dt''$$

For $|R|^2=1$ we have

$$\Pi(\Delta I)=4|\alpha|^2\sum_l\frac{\sin(\xi_l\tau)^2}{\xi_l^2}\Big(f_1^*f_2^*e^{2i\phi}+f_1f_2e^{-2i\phi}+1+2|f_2|^2\Big)+4\sum_l\frac{\sin(\xi_l\tau)^2}{\xi_l^2}|f_2|^2 \tag{B.1}$$

For $|R|^2=0$ we have

$$\Pi(\Delta I)=4\sum_l\frac{\sin(\xi_l\tau)^2}{\xi_l^2}|f_2|^2. \tag{B.2}$$

Where $\xi_l\equiv\omega_\alpha-\omega_l$, it is also $\xi_l=\delta\Omega_l$.

Finally, simplifying these equations using the definitions from $f_1 \equiv \frac{1+\mu^2+\Omega^2}{A}$ and $f_2 \equiv \frac{2\mu}{A}$, where $A \equiv (1-i\Omega)^2 - \mu^2$, and μ is the pumping parameter, we have

$$\begin{aligned} f_1^*(\Omega_l) f_2^*(\Omega_l) e^{2i\phi} + f_1(\Omega_l) f_2(\Omega_l) e^{-2\phi} &= \frac{4\mu\cos(2(\theta+\phi))\left(\mu^2+\Omega_l^2+1\right)}{\mu^4+2\mu^2\left(\Omega_l^2-1\right)+\left(\Omega_l^2+1\right)^2} \\ f_2^*(\Omega_l) f_2(\Omega_l) &= \frac{4\mu^2}{\mu^4+2\mu^2\left(\Omega_l^2-1\right)+\left(\Omega_l^2+1\right)^2} \end{aligned}$$

Therefore, for $|R|^2 = 1$, we have two cases, for $\cos(2(\theta+\phi)) = 1$ we have the anti-squeezing:

$$\Pi(\Delta I) = 4|\alpha|^2 \sum_l \frac{\sin^2(\xi_l \tau)}{\xi_l^2}\Big(1 + \frac{4\mu}{(1-\mu)^2+\Omega_l^2}\Big). \tag{B.3}$$

And for $\cos(2(\theta+\phi)) = -1$ we have the squeezing:

$$\Pi(\Delta I) = 4|\alpha|^2 \sum_l \frac{\sin^2(\xi_l \tau)}{\xi_l^2}\Big(1 - \frac{4\mu}{(1+\mu)^2+\Omega_l^2}\Big) \tag{B.4}$$

In these equations, I have neglected the term $4\sum_l \frac{\sin(\xi_l\tau)^2}{\xi_l^2}|f_2|^2$ because $|\alpha|^2 \gg 1$.